



SYMPOSIUM DUBROVNIK 2007

## Concrete Structures - - STIMULATORS OF DEVELOPMENT

Dubrovnik | Croatia | 20-23 May 2007

Topic 4: Advanced analysis of concrete structures

### EXPERIMENTAL INVESTIGATION ON THE LOAD-CARRYING CAPACITY OF THIN WEBS INCLUDING POST-TENSIONING TENDONS

Miguel Fernández Ruiz\*, Aurelio Muttoni\*\* & Eckart Hars\*\*\*

\*Ph D, IS-BETON, Ecole Polytechnique Fédérale de Lausanne  
CH-1015 Lausanne, Switzerland, miguel.fernandezruiz@epfl.ch

\*\*Professor, IS-BETON, Ecole Polytechnique Fédérale de Lausanne  
CH-1015 Lausanne, Switzerland, aurelio.muttoni@epfl.ch

\*\*\*Ph D, Grontmij, Stockholm, Sweden, eckart.hars@carlbro.se

**Key words:** Post-tensioning tendon, shear strength, testing, web, concrete crushing, bridge girder

**Abstract:** *The presence of post-tensioning tendons in webs decreases the load-carrying capacity of the compression struts that are necessary to transfer shear forces. This effect has been known for a long time, but was initially not included in design codes. In particular, older bridge designs often included fairly large ducts in rather thin webs. This paper presents the results of an extensive experimental investigation on the effect of the presence of post-tensioning ducts on the shear capacity of thin-webbed post-tensioned girders. The study included a series of large-scale tests performed in the laboratory on post-tensioned girders extracted from an existing bridge.*

## 1. INTRODUCTION

Since the 1970's, a series of investigations were conducted on the influence of post-tensioning ducts and cracking on the shear strength of post-tensioning beams. Following this research, in the 1980's and especially in the 1990's stricter requirements concerning the shear strength of post-tensioned members were introduced in most codes of practice. Currently, the design of such elements is performed by reducing the actual width of the web ( $b_w$ ) to an effective one ( $b_{eff}$ ) to account for these phenomena. This reduction is performed by means of two strength reduction factors (see Fig. 1):  $\eta_D$  accounting for the effect of duct type and size and  $\eta_\varepsilon$  accounting for transverse cracking (typically adopted as 0.60 in webs). A multiplicative formulation is usually adopted to consider their interaction.

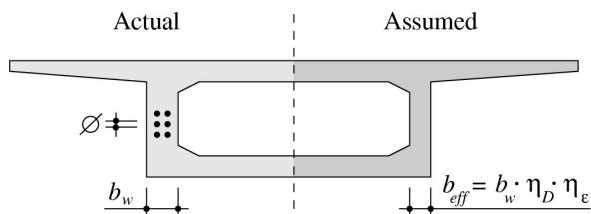


Figure 1: Post-tensioned girder webs: actual ( $b_w$ ) and effective ( $b_{eff}$ ) web width

This approach leads to safe designs<sup>1</sup> and is simple to use for the dimensioning of new structures. However, the shear strength assessment of existing bridges, especially those built before 1970 and whose original design did not consider these effects, becomes sometimes problematic. This is the reason why, a series of experimental campaigns and theoretical works have recently been performed at the Ecole Polytechnique Fédérale de Lausanne (EPFL) on this topic.

Both the influence of ducts<sup>2,3</sup> (including the recently-available plastic ducts) and the behaviour of thin-webbed members<sup>4,5</sup> have been investigated. This paper presents some results of an experimental campaign performed on actual bridge girders with the aim of investigating the behaviour and strength of thin-webbed post-tensioned beams. Detailed information of the tests performed can be found in referenced publication<sup>4</sup>.

## 2. EXPERIMENTAL CAMPAIGN

Five specimens were extracted from the beams of a five-span continuous girder bridge built in Capolago (Switzerland) in 1967 and replaced after 36 years of service. The specimens were carried to the EPFL where they were tested to failure, see Fig. 2.

Prestressed precast elements were used in the web of the original beams in combination with a cast *in situ* reinforced concrete deck slab. The bridge was longitudinally post-tensioned by two 60-mm diameter tendons, each tendon consisting of 27 wires 7-mm diameter in a metallic duct. At the time of testing, the remaining stress in the tendons was 530 MPa, only 45 % of the original post-tensioning stress<sup>1</sup>. The test specimens (16.50 m long) were extracted from the original beams (20.0 m span) as shown in Fig. 3a,b. The beams had a very small web thickness ( $b_w = 125$  mm) and a web reinforcement ratio  $\rho_w = 0.63$  %.



Figure 2: Testing of the bridge girders at EPFL

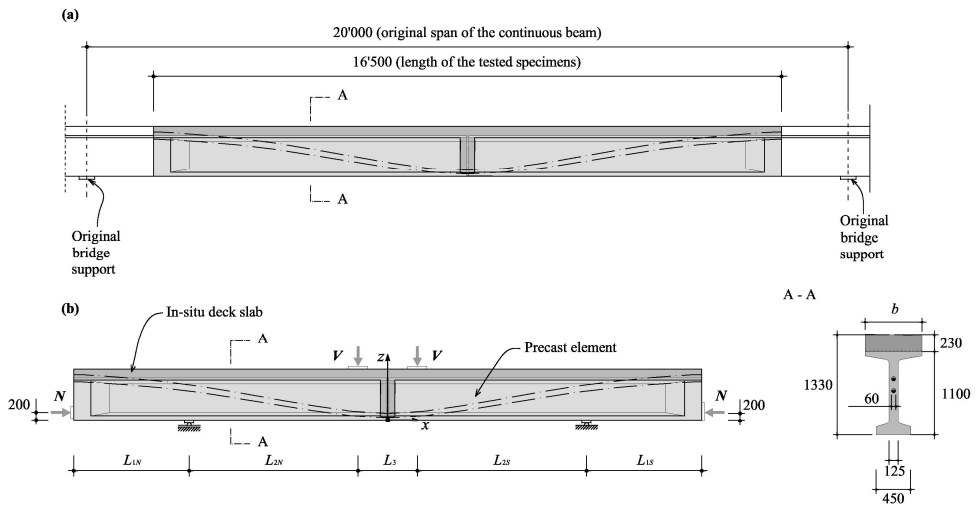


Figure 3: Tested specimens, dimensions in [mm]: (a) main dimensions of the original bridge and of the extracted specimens; and (b) test setup and cross-section detail

It must be noted that the tested specimens were simply supported beams, contrary to the continuous beams of the original bridge. Thus, in addition to the shear force applied ( $V$ ), an axial force ( $N$ ) was also applied during the test to prevent a flexural failure. The geometry of the various specimens together with the loads at failure are detailed in Table 1. All specimens failed in shear by web crushing along the post-tensioning tendons.

| Test | $L_{1N}$ [m] | $L_{1S}$ [m] | $L_{2N}$ [m] | $L_{2S}$ [m] | $L_3$ [m] | $V$ [MN] | $N$ [MN] |
|------|--------------|--------------|--------------|--------------|-----------|----------|----------|
| SH1  | 3.03         | 4.44         | 1.56         | 4.44         | 3.03      | 1.49     | 3.58     |
| SH2  | 1.83         | 4.44         | 3.96         | 4.44         | 1.83      | 1.26     | 2.02     |
| SH3  | 3.03         | 4.44         | 1.56         | 4.44         | 3.03      | 1.53     | 3.76     |
| SH4a | 1.00         | 3.23         | 0.84         | 10.73        | 0.70      | 1.12     | 0.69     |
| SH4b | 4.25         | 8.38         | 0.84         | 2.33         | 0.70      | 1.67     | 2.45     |
| SH5  | 2.43         | 4.80         | 2.04         | 3.60         | 3.63      | 1.66     | 2.98     |

Table 1: Geometric parameters and failure loads for the tested specimens

An extensive testing campaign was performed to gather information on the material properties of the beams (detailed values for each specimen can be found in [4]). The compressive strength of concrete was measured by extracting cylinders and prisms from the actual girders. A mean concrete strength  $f_{cm} = 53$  MPa was obtained in the deck slab and  $f_{cm} = 52$  MPa in the precast elements. Also, testing was performed on the various reinforcing and prestressing steels of the deck slab and of the precast elements. Hot-rolled reinforcing steel was found in the deck slab of the bridge ( $f_{ym} = 379$  MPa,  $f_{tm} = 541$  MPa) whereas cold-worked steel was found in the precast elements ( $f_{ym} = 603$  MPa,  $f_{tm} = 738$  MPa). The yield strength and tensile strength for the post-tensioning wires were  $f_{ym} = 1457$  MPa and  $f_{tm} = 1738$  MPa respectively, being  $f_{ym} = 1340$  MPa and  $f_{tm} = 1707$  MPa for the pre-tensioning wires.

### 3. TEST RESULTS OF SPECIMEN SH2

In this section, the results of the representative specimen SH2 are presented. The loading pattern and the load-midspan deflection curve are plotted in Fig. 4. It can be noted that the longitudinal axial force was applied only after a significant shear force was already present. This loading pattern allowed to investigate the structural response of the members for both small and large axial load levels. Since the axial force applied to the specimen prevented a flexural failure, a brittle shear failure developed in the specimen. The failure occurred by crushing of the concrete of the inclined compression field in the web along the post-tensioning tendons with spalling of the concrete cover, see Fig. 5.

Strain measurements were performed on the specimen during the test. Fig. 6 plots the longitudinal and vertical strain profiles for various cross-sections and load levels. Strain localization can be noted, especially close to failure, in the longitudinal strain profiles (Fig. 6a) at the level of the tendons (where the sections do not remain plane). The disturbance introduced by the tendons is also remarkable in the vertical strain profiles (Fig. 6b). At failure, vertical strains larger than 4 ‰ were measured, indicating extensive stirrup yielding.

The role of the tendons in the structural response of the member is also confirmed by the plot of the principal compressive strain directions of the web, see Fig. 7. For small values of the axial force (Fig. 7a), a strong deviation of the principal strain direction is observed at the level of the tendons. This deviation can be explained by the increase in the tendon stress due to bond. Close to failure, however, the deviation at the level of the tendons is less significant since most part of the shear force is introduced in the support region thanks to the horizontal axial force (see Fig. 7b).

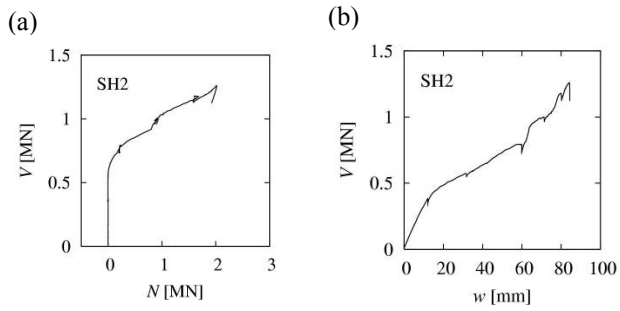


Figure 4: Test SH2: (a) loading pattern; and (b) load-midspan deflection

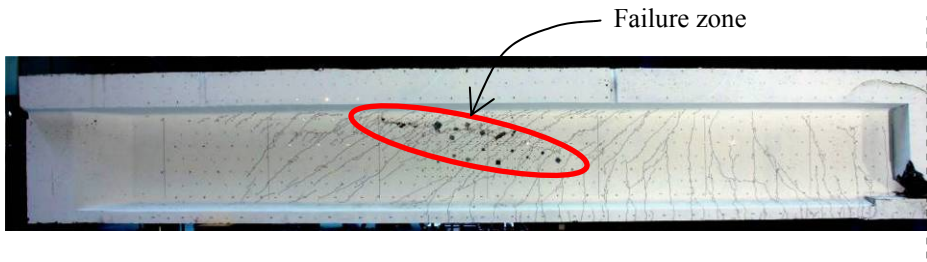


Figure 5: Failure zone of specimen SH2

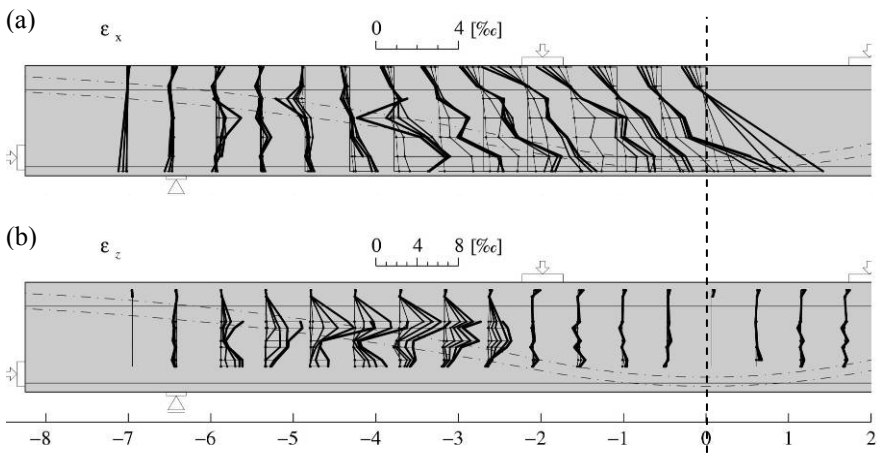


Figure 6: Measured strains at various cross-sections and load levels: (a) longitudinal strains; and (b) vertical strains

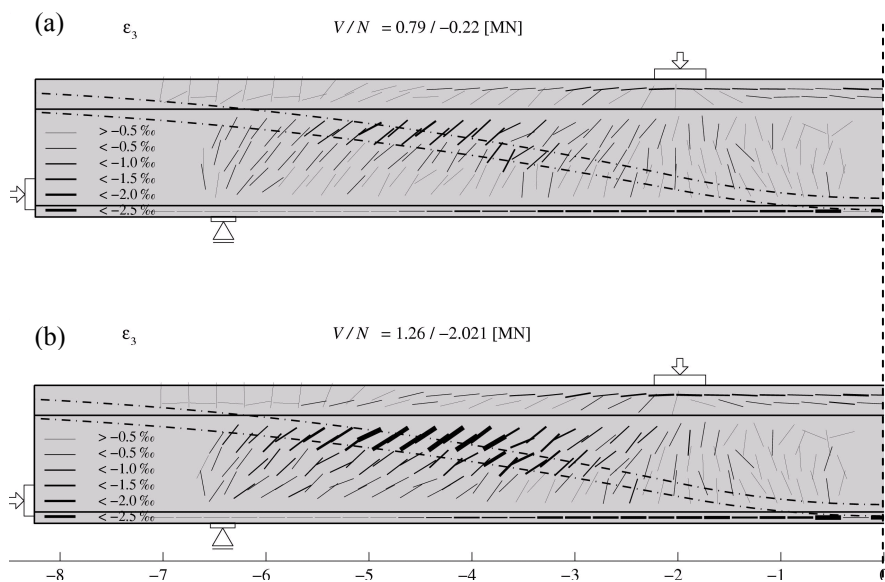


Figure 7: Measured principal compressive strain direction in the web of the beam at two load levels: (a) with limited axial force; and (b) close to failure

Other important result that can be noted in Fig. 7 is the very small angle of the compression field developing in the web. For specimen SH2, this value was around  $25^\circ$  but values around  $20^\circ$  for the principal compressive strain direction were consistently measured for various specimens tested. Also, a non-negligible inclination in the compression chord (see deck slab of Figs 7a,b) was also measured. The vertical component of the inclined compression chord can carry a non-negligible fraction of the total applied shear<sup>1</sup>.

Analyses performed using deviated stress fields [5] confirm such small values for the compression field angle. For specimen SH2, a deviated stress field can be developed [1] considering a multiplicative formulation to account for the interaction between  $\eta_D$  (0.76 according to referenced publication<sup>2</sup>) and  $\eta_\epsilon$  (set to 0.60 according to referenced publication<sup>3</sup>) leading to a theoretical failure load of  $V = 1.26$  MN (equal to the actual one) and to a compression field angle of  $25.4^\circ$ . These results confirm the validity of the multiplicative approach commonly adopted between  $\eta_D$  and  $\eta_\epsilon$ .

#### 4. BOND STRENGTH

Due to the significant role of bond between the post-tensioning wires and the surrounding concrete on the structural response of the specimens, the value of the bond strength was investigated in the test campaign. Strain measurements of the tendons made during tests SH4a and SH4b, as well as the residual strains measured after the tests by cutting the tendons, allowed to estimate the stresses in the tendons<sup>4</sup>. It was also known that the stress of the post-tensioning wires was zero at the end of the specimens because the test specimens (and thus the post-tensioning tendons) were cut from the actual girders of the

bridge. The measured stresses (see Fig. 8) are almost aligned along a straight line passing by zero at the end of the beam.

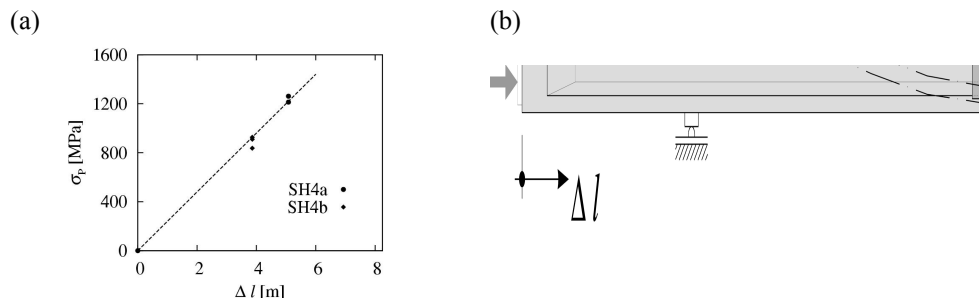


Figure 8: (a) Estimated stresses in the tendons and linear approximation; and (b) measurements position

Since a straight line gives a good estimate of the stress in the tendons, the bond stress can be assumed approximately constant. Its value can be derived from the slope of the previous line, with  $\Delta\sigma_p/\Delta l = 2 \cdot \tau_{bp}/(A_p/\pi)^{1/2}$  (where  $A_p$  is the area of the tendons), and a bond strength  $\tau_{bp} = 0.15 \cdot f_{cm}^{2/3}$  is obtained (dotted line in Figure 8). This value is small when compared to those obtained by other researchers (for instance, Zwicky proposes in [6] a bond strength of  $\tau_{bp} = 0.33 \cdot f_{cm}^{2/3}$ ). However, the value obtained is reasonable because smooth wires were used in the post-tensioning tendons.

## 5. CONCLUSIONS

This paper presents some results of an experimental campaign performed with the aim of investigating the actual behaviour of thin-webbed post-tensioned members. The main conclusions of the experimental work are:

1. Because bending failure was prevented, failure developed in all specimens by crushing of the web along the post-tensioning tendons with strong strain localization. Spalling of the concrete occurred at the failure zone.
2. Very small values (around  $20^\circ$ ) of the angle of the compression field developing in the web were measured during the test campaign.
3. The measured inclination of the compression chord developing in the deck slab indicates that a fraction of the total shear can be carried by this effect.
4. The validity of the multiplicative approach to consider the interaction between the strength reduction factors accounting for the effect of duct type and size and of the cracking state in the web is confirmed by the test results.
5. Small values of the bond strength have been measured (approximately one half of the usual values). This may be explained by the fact that smooth tendons were used

## ACKNOWLEDGEMENT

Financial support from the Swiss Federal Roads Authority is gratefully acknowledged.

## NOTATION

|                    |  |
|--------------------|--|
| $b_w, b_{eff}$     | = actual and effective web width, resp.                        |
| $f_{cm}$           | = mean compressive strength of concrete                        |
| $f_{ym}$           | = mean yield strength of steel                                 |
| $f_{tm}$           | = mean rupture strength of steel                               |
| $w$                | = mid-span deflection  |
| $x, z, l$          | = coordinates  |
| $A_p$              | = total area of post-tensioning tendons                        |
| $N, V$             | = axial and shear force, resp.                                 |
| $L$                | = length   |
| $\varepsilon_x$    | = longitudinal strain  |
| $\varepsilon_z$    | = vertical strain  |
| $\varepsilon_3$    | = principal compressive strain                                 |
| $\eta_D$           | = strength reduction factor accounting for duct type and size  |
| $\eta_\varepsilon$ | = strength reduction factor accounting for transverse cracking |
| $\rho_w$           | = web reinforcement ratio                                      |
| $\sigma_p$         | = stress in the post-tensioning tendons                        |
| $\tau_{bp}$        | = bond strength  |

## REFERENCES

- [1] Fernández Ruiz, M., Hars, E. & Muttoni, A. 2006. Shear strength of thin-webbed post-tensioned girders (in French: Résistance à l'effort tranchant des poutres précontraintes à âme mince). *Département fédéral des transports, des communications et de l'énergie, Office fédéral des routes, Rapport 606*: 68 p.
- [2] Muttoni, A., Burdet, O. L. & Hars, E. 2006. Effect of duct type on shear strength of thin webs. *ACI Structural Journal*, V. 103, No. 5: 729-735.
- [3] Hars, E. & Muttoni, A. 2006. Tests on concrete prisms on the effect of post-tensioning ducts (in German: Prismenversuche zur Untersuchung der Spanngliedpräsenz). *Test report, IS-BETON, Ecole Polytechnique Fédérale de Lausanne*: 12 p. (this test report can be downloaded from: <http://is-beton/Publications/2006/Hars06a.pdf>).
- [4] Hars, E. & Muttoni, A. 2006. Shear tests on thin-webbed post-tensioned beams (in French: Essais à l'effort tranchant sur des poutres précontraintes à âme mince). *Test report, IS-BETON, Ecole Polytechnique Fédérale de Lausanne*: 108 p. (this test report can be downloaded from: <http://is-beton/Publications/2006/Hars06.pdf>).
- [5] Muttoni, A., Schwartz, J. & Thürlimann, B. 1997. *Design of concrete structures with stress fields*: 145 p. Basel, Boston and Berlin, Switzerland: Birkhäuser.
- [6] Zwicky, D. 2002. *Strength of strongly post-tensioned concrete beams (in German: Zur Tragfähigkeit stark vorgespannter Betonbalken)*, PhD. Thesis: 228 p. Institut für Baustatik und Konstruktion, ETH Zürich.